

Multiqubit quantum phase gate using four-level superconducting quantum interference devices coupled to superconducting resonator

Muhammad Waseem,¹ Muhammad Irfan,¹ and Shahid Qamar¹

¹*Department of Physics and Applied Mathematics,
Pakistan Institute of Engineering and Applied Sciences, Nilore, Islamabad, Pakistan*
(Dated: December 24, 2012)

In this paper, we propose a scheme to realize three-qubit quantum phase gate of one qubit simultaneously controlling two target qubits using four-level superconducting quantum interference devices (SQUIDs) coupled to a superconducting resonator. The two lowest levels $|0\rangle$ and $|1\rangle$ of each SQUID are used to represent logical states while the higher energy levels $|2\rangle$ and $|3\rangle$ are utilized for gate realization. Our scheme does not require adiabatic passage, second order detuning, and the adjustment of the level spacing during gate operation which reduce the gate time significantly. The scheme is generalized for an arbitrary n -qubit quantum phase gate. We also apply the scheme to implement three-qubit quantum Fourier transform.

key words: quantum phase gate, superconducting quantum interference devices (SQUIDs), superconducting resonator, quantum Fourier transform

PACS numbers: 85.25.Dq, 85.25.-j, 03.67.Ac

I. INTRODUCTION

Quantum information processing has the potential ability to simulate hard computational problems much more efficiently than classical computers. For example factorization of large integers [1], searching for an item from disordered data base [2], and phase estimation [3]. Quantum logical gates based on unitary transformations are building blocks of quantum computer. **The schemes for realizing two-qubit quantum logical gates** using physical qubits such as atoms or ions in cavity QED [4, 5], superconducting devices like Josephson junctions [6], cooper pair boxes [7] have been proposed. In earlier studies, strong coupling with charge qubits [8] and flux qubits [9] was predicted in circuit QED. In some recent studies, experimental demonstration of strong coupling in microwave cavity QED with superconducting qubit [10–12] has been realized. The results of these experiments make superconducting qubit cavity QED an attractive approach for quantum information processing.

Among the superconducting state qubits, SQUIDs are promising candidate to serve as a qubit [13]. They have long decoherence time of the order of 1 to $5\mu s$ [14, 15], design flexibility, large-scale integration, and compatibility to conventional electronics [14, 16, 17]. They can be easily embedded in the cavity while atoms or ions require trapping techniques. Some interesting schemes for the realization of two-qubit quantum controlled phase gates based on a cavity QED technique with SQUIDs have been proposed [18–21]. These studies open a way of realizing physical quantum information processing with SQUIDs in cavity QED.

Recently, physical realization of the multiqubit gates has gained a lot of interest [22–25]. Algorithms for quantum computing become complex for large qubit system. However, multiqubit quantum phase gate reduces their complexity and can lead to faster computing. Multiqubit quantum controlled phase gate has great importance for realizing quantum-error-correction protocols [26], constructing quantum computational networks [27] and implementing quantum algorithms [28].

In this paper, we present a scheme for the realization of three-qubit quantum controlled phase gate of one-qubit simultaneously controlling two qubits using four-level SQUIDs coupled to a superconducting resonator. It may be mentioned that in an earlier study, a proposal for multiqubit phase gate of one qubit simultaneously controlling n qubits in a cavity has been presented [24], which is based upon system-cavity-pulse resonant Raman coupling, system-cavity-pulse off-resonant Raman coupling, system-cavity off-resonant interaction and system-cavity resonant interaction. In another study [25], a multiqubit phase gate based upon the tuning of the qubit frequency or resonator frequency is proposed. These proposals are quite general which can be applied to flux qubit systems or SQUIDs too. The present scheme is based on system-cavity-pulse resonant and system-cavity off-resonant interactions which can be realized using flux qubit (SQUID) system. In this proposal, two lowest levels $|0\rangle$ and $|1\rangle$ of each SQUID are used to represent the logical states while higher energy levels $|2\rangle$ and $|3\rangle$ are utilized for gate realization. A single photon is created by resonant interaction of cavity field with $|2\rangle \leftrightarrow |3\rangle$ transition of the control SQUID. In the presence of single photon inside the cavity, off-resonant interaction between the cavity field and $|2\rangle \leftrightarrow |3\rangle$ transition of each target SQUID induces a phase shift of $e^{i\theta_n}$ to each n th target SQUID. Our scheme has following advantages:

(1) Controlled phase gate operation can be performed without adjusting level spacing during gate operation, thus decoherence due to tuning of SQUID level spacing is avoided.

(2) The proposal does not require slowly changing Rabi frequencies (to satisfy adiabatic passage) and use of second-order detuning (to achieve off-resonance Raman coupling between two relevant levels), thus the gate is significantly faster.

(3) During the gate operation, tunneling between the levels $|1\rangle$ and $|0\rangle$ is not needed. The decay of level $|1\rangle$ can be made negligibly small via prior adjustment of the potential barrier between the levels $|1\rangle$ and $|0\rangle$ [29]. Therefore, each qubit can have much longer storage time.

(4) We do not require identical coupling constants of each SQUID with the resonator. Similarly, detuning of the cavity modes with the transition of the relevant levels in every target SQUID is not identical, therefore, our scheme is tolerable to inevitable non-uniformity in device parameters.

The scheme is generalized to realize n-qubit quantum controlled phase gate. Finally, it is shown that the proposed scheme can be used to implement three-qubit quantum Fourier transform(QFT).

II. QUANTUM PHASE GATE

The transformation for three-qubit quantum phase gate with one qubit simultaneously controlling two target qubits is given by

$$U_3 |q_1, q_2, q_3\rangle = e^{(i\theta_2 \delta_{q_1,1} \delta_{q_2,1})} e^{(i\theta_3 \delta_{q_1,1} \delta_{q_3,1})} |q_1, q_2, q_3\rangle, \quad (1)$$

where $|q_1\rangle$, $|q_2\rangle$, and $|q_3\rangle$ stand for basis states $|1\rangle$ or $|0\rangle$ for qubits 1, 2, and 3, respectively. Here $\delta_{q_1,1}$, $\delta_{q_2,1}$ and $\delta_{q_3,1}$ are the Kronecker delta functions. It is clear from Eq. (1) that in three qubit quantum phase gate when control qubit $|q_1\rangle$ is in state $|1\rangle$, phase shift $e^{i\theta_2}$ induces to the state $|1\rangle$ of the target qubit $|q_2\rangle$ and phase shift $e^{i\theta_3}$ to the state $|1\rangle$ of target qubit $|q_3\rangle$. When control qubit $|q_1\rangle$ is in state $|0\rangle$ nothing happens to the target qubits. Quantum phase gate operator in Dirac notation can be written as:

$$U_3 = |000\rangle \langle 000| + |001\rangle \langle 001| + |010\rangle \langle 010| + |011\rangle \langle 011| + |100\rangle \langle 100| \\ + e^{i\theta_3} |101\rangle \langle 101| + e^{i\theta_2} |110\rangle \langle 110| + e^{i\theta_2} e^{i\theta_3} |111\rangle \langle 111|. \quad (2)$$

The schematic circuit diagram for quantum phase gate with one qubit simultaneously controlling two target qubits is shown by circuit-1 in Fig. 1. The circuit-2 in Fig. 1 shows the two successive two-qubit controlled phase gate represented by U_2 and U_3 with shared target qubit (i.e., qubit $|q_1\rangle$) but different control qubits $|q_2\rangle$ and $|q_3\rangle$ (as shown by filled circles). The circuit-2 is known as gate decomposition method. The elements U_2 and U_3 represent controlled phase gate having phase shift $e^{i\theta_2}$ and $e^{i\theta_3}$, respectively. These circuits are equivalent to each other [24] which can provide fast implementation of QFT as discussed in Sec. VI.

III. DYNAMICS OF THE SYSTEM

Here we consider rf-SQUIDs which consists of Josephson junction enclosed by superconducting loop. The corresponding Hamiltonian is given by [30]

$$H_S = \frac{Q^2}{2C} + \frac{(\phi - \phi_x)^2}{2L} - E_J \cos\left(\frac{2\pi\phi}{\phi_0}\right), \quad (3)$$

where C and L are junction capacitance and loop inductance, respectively. Conjugate variables of the system are magnetic flux ϕ threading the ring and total charge Q on capacitor. The static external flux applied to the ring is ϕ_x and $E_J \equiv \frac{I_c \phi_0}{2\pi}$ is the Josephson coupling energy. Here I_c is critical current of Josephson junction and $\phi_0 = \frac{h}{2e}$ is the flux quantum. We consider the interaction of SQUID with cavity field and microwave pulses as discussed in the forthcoming subsections.

A. Control SQUID interaction with resonator

Control SQUID is biased properly to achieve desired four-level structure by varying the external flux [21] as shown in Fig. 2. The single-mode of the cavity field is resonant with $|2\rangle_1 \leftrightarrow |3\rangle_1$ transition of control SQUID, however, it is highly detuned from the transition between the other levels which can be achieved by adjusting the level spacing of

SQUID [18, 29]. Using interaction picture with rotating wave approximation one can write the Hamiltonian of system as [18]

$$H_1 = \hbar(g_1 a^\dagger |2\rangle_1 \langle 3| + H.c), \quad (4)$$

where a^\dagger and a are photon creation and annihilation operators for the cavity field mode of frequency ω_c . Here g_1 is the coupling constant between cavity field and $|2\rangle_1 \leftrightarrow |3\rangle_1$ transition of the control SQUID. The evaluation of initial states $|3\rangle_1 |0\rangle_c$ and $|2\rangle_1 |1\rangle_c$ under Eq. (4) can be written as

$$\begin{aligned} |3\rangle_1 |0\rangle_c &\rightarrow \cos(g_1 t) |3\rangle_1 |0\rangle_c - i \sin(g_1 t) |2\rangle_1 |1\rangle_c, \\ |2\rangle_1 |1\rangle_c &\rightarrow \cos(g_1 t) |2\rangle_1 |1\rangle_c - i \sin(g_1 t) |3\rangle_1 |0\rangle_c, \end{aligned} \quad (5)$$

where $|0\rangle_c$ and $|1\rangle_c$ are vacuum and single photon states of the cavity field, respectively.

B. Target SQUIDs interaction with the resonator

Suppose cavity field interacts off-resonantly with $|2\rangle_t \leftrightarrow |3\rangle_t$ ($t = 2, 3, \dots, n$) transition of each target SQUID (i.e., $\Delta_{c,t} = \omega_c - \omega_{32,t} \gg g_t$) while it is decoupled from the transition between any other levels as shown in Fig. 2. Here $\Delta_{c,t}$ is the detuning between $|2\rangle_t \leftrightarrow |3\rangle_t$ transition frequency $\omega_{32,t}$ of the target SQUID (t) and frequency of resonator ω_c and g_t is corresponding coupling constant. The effective Hamiltonian for the system in interaction picture can be written as [31, 32]

$$H_t = \frac{\hbar g_t^2}{\Delta_{c,t}} (|3\rangle_t \langle 3| - |2\rangle_t \langle 2|) a^\dagger a. \quad (6)$$

In the presence of single photon inside the cavity, the evolution of initial states $|2\rangle_t |1\rangle_c$ and $|3\rangle_t |1\rangle_c$ is given by

$$\begin{aligned} |2\rangle_t |1\rangle_c &\rightarrow e^{i g_t^2 t / \Delta_{c,t}} |2\rangle_t |1\rangle_c, \\ |3\rangle_t |1\rangle_c &\rightarrow e^{-i g_t^2 t / \Delta_{c,t}} |3\rangle_t |1\rangle_c. \end{aligned} \quad (7)$$

It is clear that phase shift $e^{i \frac{g_t^2 t}{\Delta_{c,t}}}$ and $e^{-i \frac{g_t^2 t}{\Delta_{c,t}}}$ is induced to the state $|2\rangle_t$ and $|3\rangle_t$ of the target SQUID. However, states $|2\rangle_t |0\rangle_c$ and $|3\rangle_t |0\rangle_c$ remain unchanged.

C. SQUID driven by microwave pulses

Let two levels $|i\rangle$ and $|j\rangle$ of each SQUID is driven by classical microwave pulse. The interaction Hamiltonian in this case is [18]

$$H_{\mu w} = \Omega_{ij} e^{i\varphi} |i\rangle \langle j| + H.c, \quad (8)$$

where Ω_{ij} is the Rabi frequency between two levels $|i\rangle$ and $|j\rangle$ and φ is the phase associated with classical field. From Eq. (8) one can get the following rotations:

$$\begin{aligned} |i\rangle &\rightarrow \cos(\Omega_{ij} t) |i\rangle - i e^{-i\varphi} \sin(\Omega_{ij} t) |j\rangle, \\ |j\rangle &\rightarrow \cos(\Omega_{ij} t) |j\rangle - i e^{i\varphi} \sin(\Omega_{ij} t) |i\rangle. \end{aligned} \quad (9)$$

In our case $|i\rangle \rightarrow |j\rangle$ transition corresponds to $|0\rangle \rightarrow |2\rangle$, $|1\rangle \rightarrow |2\rangle$ and $|1\rangle \rightarrow |3\rangle$ as shown in Figs. 3-5. It may be noted that the resonant interaction of microwave pulse with SQUID can be carried out in a very short time by increasing the Rabi frequency of pulse i.e., intensity of the pulse.

IV. THREE-QUBIT CONTROLLED PHASE GATE

Let us consider three-qubit controlled phase gate using three four-levels SQUIDs coupled to a superconducting resonator. For the notation convenience, we denote the ground level as $|1\rangle$ and first excited state as $|0\rangle$ for each target SQUID as shown in Fig. 4-5. Here we assume that the resonator mode is initially in a vacuum state. The

notation $\omega_{i,j}^n$ represents the microwave frequency in resonance with the transition frequency between $|i\rangle \leftrightarrow |j\rangle$ level of SQUID ($n = 1, 2, 3$). Here we discuss a quantum phase gate with $\theta_3 = \pi/4$ and $\theta_2 = \pi/2$.

The procedure for realizing the three-qubit controlled phase gate is divided into the following four stages of operations:

Forward resonant operation on control SQUID (1):

Step 1: Apply microwave pulse with frequency $f = \omega_{3,1}^1$ and phase $\varphi = \pi$ to the control SQUID (1). Choose time interval $t_1 = \frac{\pi}{2\Omega_{13}}$ to transform the state $|1\rangle_1$ to $i|3\rangle_1$ as shown in Fig. 3(a). The level $|3\rangle_1$ of control SQUID (1) is now occupied. Cavity field interacts resonantly to the $|2\rangle_1 \leftrightarrow |3\rangle_1$ transition of control SQUID (1) shown in Fig. 3(b). Wait for time interval $t'_1 = \pi/2g_1$ such that the transformation $|3\rangle_1|0\rangle_c \rightarrow -i|2\rangle_1|1\rangle_c$ is obtained. The overall step can be written as $|1\rangle_1|0\rangle_c \xrightarrow{t_1} i|3\rangle_1|0\rangle_c \xrightarrow{t'_1} |2\rangle_1|1\rangle_c$. However, the state $|0\rangle_1|0\rangle_c$ remains unchanged.

Step 2: Apply microwave pulse with frequency $f = \omega_{2,0}^1$ and phase $\varphi = \pi/2$ to the control SQUID (1) as shown in Fig. 3(c). We choose pulse duration $t_2 = \pi/2\Omega_{02}$ to obtain the transformation $|2\rangle_1(|0\rangle_1) \rightarrow |0\rangle_1(-|2\rangle_1)$. Here $|2\rangle(|0\rangle) \rightarrow |0\rangle(-|2\rangle)$ means the transition from $|2\rangle \rightarrow |0\rangle$ and $|0\rangle \rightarrow -|2\rangle$.

Off-resonant operation on target SQUID (2):

Step 3: Apply microwave pulse with frequency $f = \omega_{2,1}^2$ and phase $\varphi = -\pi/2$ to the SQUID (2) as shown in Fig. 4(a). We choose the pulse duration $t_3 = \pi/2\Omega_{12}$ to obtain the transformation $|1\rangle_2(|2\rangle_2) \rightarrow |2\rangle_2(-|1\rangle_2)$. It is important to mention here that, steps 2 and 3 can be performed simultaneously, by setting $\Omega_{02} = \Omega_{12}$, which makes the implementation time of both steps equal. This condition can be achieved by adjusting the intensities of the two pulses.

Step 4: After the above operation, the cavity field is in a single photon state $|1\rangle_c$, while levels $|2\rangle$ and $|3\rangle$ of the control SQUID (1) and target SQUID (3) are unpopulated. Therefore, there is no coupling of the cavity field with control SQUID (1) and target SQUID (3). The cavity field now interacts off-resonantly with $|2\rangle_2 \rightarrow |3\rangle_2$ transition of the SQUID (2) shown in Fig. 4(b). It is clear from Eq. (7) that for time $t_4 = (\pi\Delta_{c,2})/2g_2^2$ state $|2\rangle_2|1\rangle_c$ evolves to $e^{i\pi/2}|2\rangle_2|1\rangle_c$, where $\Delta_{c,2}$ represents the detuning of the relevant levels of SQUID (2) with the cavity field. However, the states $|0\rangle_2|0\rangle_c$, $|0\rangle_2|1\rangle_c$, and $|2\rangle_2|0\rangle_c$ remain unchanged.

Step 5: Apply microwave pulse with frequency $f = \omega_{2,1}^2$ and phase $\varphi = \pi/2$ to the SQUID (2) as shown in Fig. 4(c). The transformation $|1\rangle_2(|2\rangle_2) \rightarrow -|2\rangle_2(|1\rangle_2)$ is obtained by choosing the pulse duration $t_5 = \pi/2\Omega_{12}$.

Off-resonant operation on target SQUID (3):

Step 6: Apply microwave pulse with frequency $f = \omega_{3,1}^3$ and phase $\varphi = -\pi/2$ to the target SQUID (3) as shown in Fig. 5(a). The transformation $|1\rangle_3(|2\rangle_3) \rightarrow |2\rangle_3(-|1\rangle_3)$ is obtained by choosing the pulse duration $t_6 = \pi/2\Omega_{12}$. One can see that steps 5 and 6 can be performed simultaneously, in a similar fashion as mentioned earlier.

Step 7: After the above operation, when the cavity field is in a single photon state $|1\rangle_c$, the levels $|2\rangle$ and $|3\rangle$ of control SQUID (1) and target SQUID (2) are unpopulated. Under this condition, SQUIDS (1) and (2) no longer interact with the cavity field. However, cavity field interacts off-resonantly to $|2\rangle_3 \rightarrow |3\rangle_3$ transition of the target SQUID (3) as shown in Fig. 5(b). It is clear from Eq. (7) that for $t_7 = (\pi\Delta_{c,3})/4g_3^2$ state $|2\rangle_3|1\rangle_c$ evolves to $e^{i\pi/4}|2\rangle_3|1\rangle_c$, where $\Delta_{c,3}$ represents the detuning between the relevant levels of SQUID (3) and cavity field. However, the states $|0\rangle_3|0\rangle_c$, $|0\rangle_3|1\rangle_c$, and $|2\rangle_3|0\rangle_c$ remain unchanged.

Step 8: Apply microwave pulse with frequency $f = \omega_{3,1}^3$ and phase $\varphi = \pi/2$ to the SQUID (3) as shown in Fig. 5(c). The transformation $|1\rangle_3(|2\rangle_3) \rightarrow -|2\rangle_3(|1\rangle_3)$ is obtained by choosing the pulse duration $t_8 = \pi/2\Omega_{12}$.

Backward resonant operation on control SQUID (1):

Step 9: Apply microwave pulse with frequency $f = \omega_{2,0}^1$ and phase $\varphi = -\pi/2$ to the control SQUID (1) shown in Fig. 3(c). We choose pulse duration $t_9 = \pi/2\Omega_{02}$ to transform state $|2\rangle_1(|0\rangle_1) \rightarrow -|0\rangle_1(|2\rangle_1)$ for SQUID (1). Again steps 8 and 9 can be performed, simultaneously.

Step 10: Now control SQUID (1) is in state $|2\rangle$ while levels $|2\rangle$ and $|3\rangle$ of target SQUIDS are unpopulated when cavity field is in a single photon state $|1\rangle_c$. Under this condition, both target SQUIDS no longer interact with the cavity field. Perform an inverse operation of step(1) i.e., wait for time interval $t'_1 = \pi/2g_1$ during which resonator interacts resonantly to the $|2\rangle_1 \leftrightarrow |3\rangle_1$ transition of control SQUID (1) such that transformation $|2\rangle_1|1\rangle_c \rightarrow -i|3\rangle_1|0\rangle_c$ is obtained (Fig. 3(b)). Then apply microwave pulse with frequency $f = \omega_{3,1}^1$ and phase $\varphi = \pi$ to the control SQUID (1). Choose the time interval $t_1 = \frac{\pi}{2\Omega_{13}}$ to transform the state $|3\rangle_1$ to $i|1\rangle_1$ as shown in Fig. 3(a). The over all step can be written as $|2\rangle_1|1\rangle_c \xrightarrow{t'_1} -i|3\rangle_1|0\rangle_c \xrightarrow{t_1} |1\rangle_1|0\rangle_c$. However, the state $|0\rangle_1|0\rangle_c$ remains unchanged. The states of the whole system after each step of the above mentioned operations can be summarized as

achieved with resonator mode returning to original vacuum state through a sequence of operations **given by**

$$U_n = U_{\mu w}^{(1)}(\pi) \otimes U_r^{(1)}(\pi/2g_1) \otimes (U_{\mu w}^{(1)}(\pi/2))^\dagger \otimes \prod_{t=2}^n [U_{\mu w}^{(t)}(\pi/2) \otimes U^{(t)}(\theta_t) \otimes (U_{\mu w}^{(t)}(\pi/2))^\dagger] \\ \otimes U_{\mu w}^{(1)}(\pi/2) \otimes U_r^{(1)}(\pi/2g_1) \otimes U_{\mu w}^{(1)}(\pi), \quad (12)$$

where $t = 2, 3, \dots, n$ stands for target SQUID and $\prod_{t=2}^n U^{(t)} = U^{(n)} \otimes \dots \otimes U^{(3)} \otimes U^{(2)}$ shows off-resonant operation on each target SQUID.

The two-qubit controlled phase gate can easily be obtained from Eq. (12) by choosing $n = 2$. In this case Eq. (12) reduces to the following:

$$U_2 = U_{\mu w}^{(1)}(\pi) \otimes U_r^{(1)}(\pi/2g_1) \otimes (U_{\mu w}^{(1)}(\pi/2))^\dagger \otimes U_{\mu w}^{(2)}(\pi/2) \otimes U^{(2)}(\theta_2) \otimes (U_{\mu w}^{(2)}(\pi/2))^\dagger \\ \otimes U_{\mu w}^{(1)}(\pi/2) \otimes U_r^{(1)}(\pi/2g_1) \otimes U_{\mu w}^{(1)}(\pi). \quad (13)$$

It is clear that we need to apply forward resonant operation on control SQUID to create single photon in the cavity. Then phase shift of $e^{i\pi}$ is induced on target SQUID by choosing interaction **time** $t = \frac{\pi\Delta_{c,2}}{g_2^2}$ during off-resonant operation. After backward resonant operation on control SQUID, we obtain two qubit controlled phase gate in five steps [21]. The number of steps required to implement n qubit phase gate are $2n + 1$. It may be mentioned that the number of steps required to implement an equivalent n qubit decomposed phase gate are $5(n - 1)$.

VI. QUANTUM FOURIER TRANSFORM(QFT)

The factorization of composite number via Shor's algorithm [1] is an interesting example of quantum information processing. Quantum Fourier transform lies at the heart of Shor's algorithm. Quantum Fourier transform is a linear operator that transforms an orthogonal basis $|k\rangle$ into superposition given by

$$|k\rangle \rightarrow \frac{1}{\sqrt{2^n}} \sum_{j=0}^{2^n-1} e^{i2\pi jk2^{-n}} |j\rangle, \quad (14)$$

where n is the number of qubits. The combination of single qubit rotations and two qubit quantum phase gate form a complex network to implement QFT for higher qubits. For example, see circuit-1 in Fig. 6 for three qubit QFT. However, the implementation scheme can be simplified by using equivalent circuit as shown in Fig. 1. For three-qubit QFT, single-qubit Hadamard transformation, two-qubit controlled phase gate, and three qubit quantum controlled phase gate of one qubit, simultaneously controlling two target qubits are needed as shown by circuit-2 in Fig.6. The QFT can be accomplished in following 5 stages:

Stage(1) Apply the Hadamard gate on SQUID (3). The Hadamard rotation brings logical qubit $|0\rangle$ and $|1\rangle$ into superposition state i.e. $|0\rangle \rightarrow \frac{1}{\sqrt{2}}(|0\rangle + |1\rangle)$ and $|1\rangle \rightarrow \frac{1}{\sqrt{2}}(|0\rangle - |1\rangle)$. Hadamard gate can be accomplished through two step process that involves an auxiliary level $|3\rangle$ via method described in Ref [34]. We need two microwave pulses of different frequencies. One is resonant to $|0\rangle \leftrightarrow |3\rangle$ transition frequency and other is resonant to $|1\rangle \leftrightarrow |3\rangle$ transition frequency. Hadamard transformation can be realized through following three steps:

Step (a) Apply microwave pulse with frequency $f = \omega_{1,3}^3$ and phase $\varphi = \pi/2$ to SQUID (3). We choose pulse duration $t = \pi/2\Omega_{13}$ to transform state $|1\rangle \rightarrow -|3\rangle$ while state $|0\rangle$ remains unchanged.

Step (b) Apply microwave pulse with frequency $f = \omega_{0,3}^3$ and phase $\varphi = -\pi/2$ to SQUID (3). We choose pulse duration $t = \pi/4\Omega_{13}$ to obtain the transformation $|0\rangle \rightarrow \frac{1}{\sqrt{2}}(|0\rangle + |3\rangle)$ and $|3\rangle \rightarrow \frac{1}{\sqrt{2}}(-|0\rangle + |3\rangle)$.

Step (c) Repeat the operation described in step (a) on SQUID (3) to obtain the transformation $|3\rangle \rightarrow |1\rangle$ while state $|0\rangle$ remains unchanged. The above operations are summarized as

$$|0\rangle \xrightarrow{1} |0\rangle \xrightarrow{2} \frac{1}{\sqrt{2}}(|0\rangle + |3\rangle) \xrightarrow{3} \frac{1}{\sqrt{2}}(|0\rangle + |1\rangle) \\ |1\rangle \xrightarrow{1} -|3\rangle \xrightarrow{2} \frac{1}{\sqrt{2}}(|0\rangle - |3\rangle) \xrightarrow{3} \frac{1}{\sqrt{2}}(|0\rangle - |1\rangle). \quad (15)$$

Stage (2) Adjust the level spacing of SQUID (3) so that transition between levels $|2\rangle_3$ and $|3\rangle_3$ is resonant to the cavity field. It acts as a control qubit. Then apply resonant forward operation on SQUID (3). A single photon is created in the cavity which induces a phase shift of $e^{i\frac{\pi}{2}}$ on SQUID (2) through off-resonant operation.

Stage (3) Repeat the same operations described in stage (1) on SQUID (2).

Stage (4) Readjust the level spacing of SQUID (3), so that its relevant levels becomes off-resonant to the cavity field to apply three-qubit controlled phase gate with SQUID (1) simultaneously controlling SQUID (2) and SQUID (3) through operations described in Sec. IV.

Stage (5) Repeat the same operations described in stage (1) on SQUID (1).

Proceeding in a similar way, the proposed scheme can also be generalized up to arbitrary n-qubit by placing n SQUIDs in a cavity. It is clear from circuit-1 in Fig. 6 that the implementation of n-qubit QFT requires n-Hadamard gates and $n(n-1)/2$ two-qubit phase gates. This shows the complexity involved in implementing QFT. The situation may become much more complicated, if complexity of calibrating and operating 4-level SQUIDs is also taken into account. However, the complexity can be reduced using quantum controlled phase gate of one qubit simultaneously controlling n target qubits [24, 33]. This is claimed only in terms of number of steps involved and implementation time required for our proposal as compared to the corresponding decomposed method.

It must be pointed out, that we need level adjustment for the implementation of three-qubit QFT. However, this level adjustment is only required before implementing stage 2 and 4 (see Fig. 6) and there is no need for level adjustment during the implementation of phase gates. Level adjustment can be controlled by varying external flux ϕ_x or critical current I_c [29]. Thus individual SQUID can be tuned in or out of resonance with cavity field.

VII. DISCUSSION

The total estimated operational time for three-qubit controlled phase gate is

$$\tau = 2t_1 + 2t'_1 + t_2 + t_4 + t_5 + t_7 + t_8. \quad (16)$$

On substituting the values of interaction times given in sect. IV, we obtained

$$\tau = \pi(1/\Omega_{13} + 1/g_1 + 3/2\Omega_{02} + \Delta_{c,2}/2g_2^2 + \Delta_{c,3}/4g_3^2). \quad (17)$$

Here we consider without loss of generality $g_1 \approx g_2 \approx g_3 \approx 3 \times 10^9 s^{-1}$ [22]. On choosing $\Delta_{c,2} = \Delta_{c,3} = 10g_3$, $\Omega_{02} \approx \Omega_{13} \approx 10g_1$, we have operational time $\tau \approx 9.16ns$. For n-qubit controlled phase gate, we have $g_m = g(m=1, 2, \dots, n)$ and total operational time is $\tau_n = \frac{\pi}{g}(\frac{22+n}{20} + \frac{10(2^{n-1}-1)}{2^{n-1}})$. However, if we follow the gate decomposition method then total operation time for the equivalent circuit is given by $\tau_n = \frac{\pi}{g}(\frac{6(n-1)}{5} + \frac{10(2^{n-1}-1)}{2^{n-1}})$. The time required to implement an equivalent decomposed three-qubit phase gate can easily be obtained from this expression, which comes out to be $\tau \approx 10.36ns$. In order to make a quantitative estimate on the speed of the two approaches, next we show the plot of the operation time as a function of number of qubits n in Fig. 7. It is clear that implementation time for the decomposed circuit increases rapidly with n as compared to the multiqubit gate. This shows that our approach is significantly faster than performing two separate two-qubit controlled phase gates which is quite interesting.

Here, we would like to make a comparison of our scheme with the earlier proposal for n-target-qubit control-phase gate (NTCP) [25]. In the earlier study [25], the phase induced on each target qubit is the same i.e., $\theta_1 = \theta_2 = \dots = \theta_n = \pi$, whereas in our proposal different phases are induced on each target qubit. However, NTCP gate can easily be realized in our scheme by using the following steps:

1. Apply step 1 of section-IV on control SQUID (1) which generates a single photon in the cavity.
2. Apply step 2 on SQUID (1), step 3 on SQUID (2), and step 6 on SQUID (3), simultaneously.
3. Apply off-resonant operation i.e., step 4 on SQUID (2) and step 7 on SQUID (3), simultaneously, to obtain phase shift of $e^{i\pi}$. This can be achieved by choosing **interaction time** $t = \frac{\pi\Delta_{c,t}}{g_t^2}$ such that $\frac{\Delta_{c,t}}{g_t^2}$ is the same for all target SQUIDs.

4. Apply step 5 on SQUID (2), step 8 on SQUID (3), and step 9 on SQUID (1), simultaneously.

5. Finally, apply step 10 on control SQUID (1), as a result single photon in the cavity is absorbed.

Here we have considered 3 qubits, however, the scheme is applicable to arbitrary number of qubits. Thus, NTCP gate can be realized in five steps which is independent of the total number of qubits. The implementation time comes out to be $12ns$.

In another study [24], the implementation of a multiqubit phase gate having different phases on all target qubits is proposed. The number of steps required to implement this scheme are independent of the number of qubits, however, the phase induced are conditional. Our proposal can also be modified to implement a multiqubit phase gate of different phases with fixed number of steps for arbitrary number of qubits. These modifications are given by the following:

1. Apply step 1 on SQUID (1) as given in section-IV.
2. Apply step 2 on SQUID (1), step 3 on SQUID (2), and step 6 on SQUID (3), simultaneously.

3. Allow both the target qubits to interact off-resonantly with the cavity mode i.e., step 4 and 7 in section IV. The evolution is governed by Eq. (7). In order to induce a phase of $\pi/2$ on SQUID (2) and $\pi/4$ on SQUID (3), we have to adjust the interaction time as $\pi\Delta_{c,2}/2g_2^2$ and $\pi\Delta_{c,3}/4g_3^2$, respectively. To implement these two steps, simultaneously, one needs both these times to be equal which can be achieved if, $\Delta_{c,2}/g_2^2 = \frac{1}{2}\Delta_{c,3}/g_3^2$. However, this condition becomes more complex with the increase in the number of qubits. For example, for a four-qubit gate it becomes $\Delta_{c,2}/g_2^2 = \frac{1}{2}\Delta_{c,3}/g_3^2$ and $\Delta_{c,3}/g_3^2 = \frac{1}{2}\Delta_{c,4}/g_4^2$, where $\Delta_{c,4}$ and g_4 correspond to the detuning and coupling of the fourth SQUID.

4. Apply step 5 on SQUID (2), step 8 on SQUID (3) and step 9 on SQUID (1), simultaneously.

5. Apply step 10 on control SQUID (1), as a result single photon in the cavity is absorbed.

It is clear that we can implement a multiqubit phase gate having different phases on each target qubit in five steps for arbitrary number of qubits.

Here, we discuss different issues related to the gate operations. The Level $|3\rangle$ of control SQUID (1) is occupied in the steps 1 and 10 as discussed in section IV, which involve the microwave pulse of frequencies ω_{13} , and SQUID resonator resonant interaction. The corresponding operational time for three-qubit controlled phase gate in step 1 or 10 is given by

$$\tau_1 = \pi(1/2\Omega_{13} + 1/2g_1). \quad (18)$$

It is clear that τ_1 can be shortened sufficiently by increasing the Rabi frequencies and coupling constant. Control SQUID (1) can be designed so that energy relaxation time of level $|3\rangle$ (γ_3^{-1}) is sufficiently long as compared to the operational time. Thus decoherence due to energy relaxation of level $|3\rangle$ is negligibly small under the condition $\gamma_3^{-1} \gg \tau_1$ [21].

The effect of dissipation during the gate operations can be neglected by considering a high-Q resonator. The direct interaction between SQUIDS can be negligible under the condition $H_{s,s} \ll H_{s,r}H_{s,\mu\omega}$ [22]. Here $H_{s,s}$ is the interaction energy between two nearest neighbor SQUIDS, $H_{s,r}$ is the interaction energy between resonator and SQUID and $H_{s,\mu\omega}$ is the SQUID microwave interaction.

When levels $|2\rangle$ and $|3\rangle$ are manipulated by microwave pulses, resonant interaction as well as off-resonant interaction between resonator mode and $|2\rangle \leftrightarrow |3\rangle$ transition of each SQUID is unwanted. This effect can be minimized by setting the condition $\Omega_{i,j} \gg g_1$ for control SQUIDS and $\Omega_{i,j} \gg g_t^2/\Delta_{c,t}$ for target SQUIDS. The level $|3\rangle$ of each target SQUID interacts off-resonantly to the cavity field during step 4 and 7. Its occupation probability needs to be negligibly small in order to reduce the gate error [21]. The occupation probability of level $|3\rangle$ for target SQUID is given by [19]

$$p_3 \approx \frac{1}{1 + \frac{\Delta_{c,t}^2}{4g_t^2}}. \quad (19)$$

For the choice of $\Delta_{c,t} = 10g_t$, we have $p_3 \approx 0.04$ which is further reducible by increasing the ratio of $\Delta_{c,t}/g_t$.

The Hadamard transformation is accomplished by two microwave pulses of different frequencies in three steps described in Sec. VI. These steps can be implemented faster by increasing the Rabi frequency of pulses. The operation time for Hadamard gate is around $5ns$ [34].

VIII. CONCLUSION

In conclusion, we have presented a scheme for the realization of three-qubit controlled phase gate with one qubit, simultaneously controlling two target qubits using four-level SQUIDS coupled to a single-mode superconducting microwave resonator. The scheme is based on the generation of a single photon in the cavity mode by resonant interaction of cavity field with $|2\rangle \leftrightarrow |3\rangle$ transition of control SQUID and introduction of phase shift $e^{i\theta_n}$ to each target SQUID by off-resonant interaction of the cavity field with $|2\rangle \leftrightarrow |3\rangle$ transition. Finally, backward resonant operation is applied which absorbs the single photon as a result field inside the microwave cavity reduces to its original vacuum state.

The proposed scheme for quantum controlled phase gate has some interesting features, for example, it does not require adjustment of level spacing during gate operation which reduces the cause of decoherence. The present scheme does not require the adiabatic passage and second order detuning which makes the gate implementation time faster. During the gate operation, tunneling between the level $|1\rangle$ and $|0\rangle$ is not employed. Prior adjustment of the potential barrier between level $|1\rangle$ and $|0\rangle$ can be made such that the decay of level $|1\rangle$ is negligibly small. Therefore, each qubit can have much longer storage time [29]. The scheme can readily be generalized to realize an arbitrary multiqubit quantum phase gate of one qubit simultaneously controlling n qubits. We have also applied the scheme to implement three-qubit quantum Fourier transform.

-
- [1] P. W. Shor, in proceedings of the 35th annual symposium on foundations of computer science, IEE Computer society press, Santa Fe, NM (1994).
 - [2] L. K. Grover, Phys. Rev. Lett. **79**, 325 (1997).
 - [3] A. Y. Kitaev, quant-ph/9511026.
 - [4] M. S. Zubairy, M. Kim, and M. O. Scully, Phys. Rev. A **68**, 033820 (2003).
 - [5] J. I Cirac and P. Zoller, Phys. Rev. Lett. **74**, 4091 (1995).
 - [6] A. Blais and A. M. Zagoskin, Phys. Rev. A **61**, 042308 (2000).
 - [7] Y. Makhlin, G. Schoen, and A. Shnirman, Rev. Mod. Phys. **73**, 357 (2001).
 - [8] A. Blais, R. S. Huang, A. Wallraff, S. M. Girvin, and R. J. Schoelkopf, Phys. Rev. A **69**, 062320 (2004).
 - [9] C. P. Yang, Shih-I. Chu, and S. Han, Phys. Rev. Lett. **92**, 117902 (2004).
 - [10] A. Wallraff, D. I. Schuster, A. Blais, L. Frunzio, R. -S. Huang, J. Majer, S. Kumar, S. M. Girvin, and R. J. Schoelkopf, Nature (London) **431**, 162 (2004).
 - [11] I. Chiorescu, P. Bertet, K. Semba, Y. Nakamura, C. J. P. M. Harmans, and J. E. Mooij, Nature (London) **431**, 159 (2004).
 - [12] H. Paik et al., Phys. Rev. Lett. **107**, 240501 (2011).
 - [13] M. F. Bocko, A. M. Herr, and M. J. Feldman, IEEE Trans. Appl. Supercond. **7**, 3638 (1997).
 - [14] Y. Yu, S. Han, X. Chu, S.-I. Chu, and Z. Wang, Science **296**, 889 (2002).
 - [15] D. Vion, A. Aassime, A. Cottet, P. Joyez, H. Pothier, C. Urbina, D. Esteve, and M. Devoret, Science **296**, 886 (2002).
 - [16] I. Chiorescu et al., Nature (London) **431**, 159 (2004).
 - [17] J. B. Majer, F. G. Paauw, A. C. J. ter Haar, C. J. P. M. Harmans, and J.E.Mooij, Phys. Rev. Lett. **94**, 090501 (2005).
 - [18] C. P. Yang, S. I. Chu, and S. Han, Phys. Rev. A **67**, 042311 (2003).
 - [19] C. P. Yang, S. I. Chu, and S. Han, Phys. Rev. A **70**, 044303 (2004).
 - [20] K. H. Song, S. H. Xiang, Q. Liu, and D. H. Lu, Phys. Rev. A **75**, 032347 (2007).
 - [21] X. L. He C. P. Yang, S. Li, J. Y. Luo, and S. Han Phys. Rev. A **82**, 024301 (2010).
 - [22] C. P. Yang and S. Han, Phys. Rev. A **72**, 032311 (2005); **73**, 032317 (2006).
 - [23] J. T. Chang and M. S. Zubairy, Phys. Rev. A **77**, 012329 (2008).
 - [24] C. P. Yang, S. B. Zheng and F. Nori Phys. Rev. A **82**, 062326 (2010).
 - [25] C. P. Yang, Y. X. Liu, and F. Nori, Phys. Rev. A **81**, 062323 (2010).
 - [26] J. Chiaverini, D. Leibfried, T. Schaetz, M. D. Barrett, R. B. Blakestad, J. Britton, W. M. Itano, J. D. Jost, E. Knill, C. Langer, R. Ozeri, and D. J. Wineland, Nature (London) **432**, 602 (2004).
 - [27] Z. diao, M. S. Zubairy, and G. Chen Z. Naturforsch., A: Phys. Sci. **57a** 701-708 (2002).
 - [28] M. S. Zubairy, A. B. Matsko, and M. O. Scully, Phys. Rev. A **65**, 043804 (2002).
 - [29] S. Han, J. Lapointe, and J. E. Lukens, Single-Electron Tunneling and Mesoscopic Devices (Springer-Verlag, Berlin, 1991), Vol. 31, pp. 219 – 222.
 - [30] S. Han, R. Rouse, and J. E. Lukens, Phys. Rev. Lett. **76**, 3404 (1996).
 - [31] S. B. Zheng and G. C. Guo, Phys. Lett. A **223**, 332 (1996).
 - [32] M. J. Holland, D. F. Walls, and P. Zoller, Phys. Rev. Lett. **67**, 1716 (1991).
 - [33] M. O. Scully and M. S. Zubairy, Phys. Rev. A **65**, 052324 (2002); M. A Nielsen and I. L. Chuang. Quantum Computing and Quantum Information. Cambridge University Press, (2000).
 - [34] C. P. Yang and S. Han, Phys. Rev. A **74**, 044302 (2006).

Caption Figure 1:

Circuit-1 shows quantum phase gate with one qubit $|q_1\rangle$ simultaneously controlling two target qubits $|q_2\rangle$ and $|q_3\rangle$. Circuit-2 shows the two successive two-qubit controlled phase gate with shared target qubit $|q_1\rangle$. The elements U_2 and U_3 represent two qubit controlled phase gate of phase shift $e^{i\theta_2}$ and $e^{i\theta_3}$, respectively. These circuits are equivalent to each other.

Caption Figure 2:

Level diagram of control SQUID and target SQUIDs with four levels $|0\rangle$, $|1\rangle$, $|2\rangle$, and $|3\rangle$. The levels $|2\rangle$, and $|3\rangle$ of control SQUID interact resonantly to resonator while levels $|2\rangle$ and $|3\rangle$ of each target SQUID interact off-resonantly to the resonator. The difference between level spacing of each SQUID can be achieved by choosing different device parameters for SQUIDs.

Caption Figure 3:

Illustration of control SQUID(1) interacting with the resonator mode and/or the microwave pulses during the gate operation.

Caption Figure 4:

Illustration of target SQUID(2) interacting with the resonator mode and/or the microwave pulses during the gate operation.

Caption Figure 5:

Illustration of target SQUID(3) interacting with the resonator mode and/or the microwave pulses during the gate operation.

Caption Figure 6:

Circuit-1 is a schematic network for three qubit QFT. The states $|q_n\rangle$ and $|k_n\rangle$ ($n = 1, 2, 3$) represent inputs and outputs, respectively. Here H represents Hadamard transformation and U_n two-qubit conditional phase transformation. The filled circles represent the control qubits. Using the equivalent circuit shown in Fig. 1., circuit-1 reduces to circuit-2.

Caption Figure 7: Plot of the gate implementation time against the number of qubits.

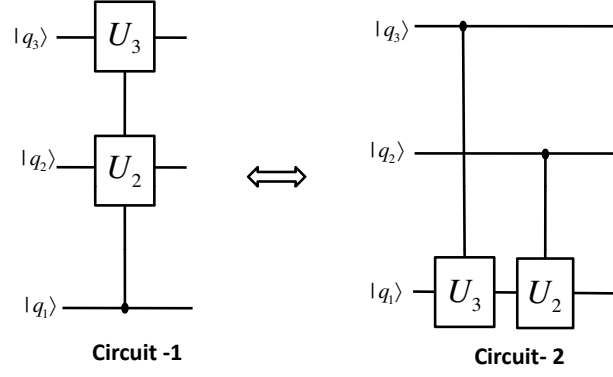


FIG. 1: Circuit-1 shows quantum phase gate with one qubit $|q_1\rangle$ simultaneously controlling two target qubits $|q_2\rangle$ and $|q_3\rangle$. Circuit-2 shows the two successive two-qubit controlled phase gate with shared target qubit $|q_1\rangle$. The elements U_2 and U_3 represent two qubit controlled phase gate of phase shift $e^{i\theta_2}$ and $e^{i\theta_3}$, respectively. These circuits are equivalent to each other.

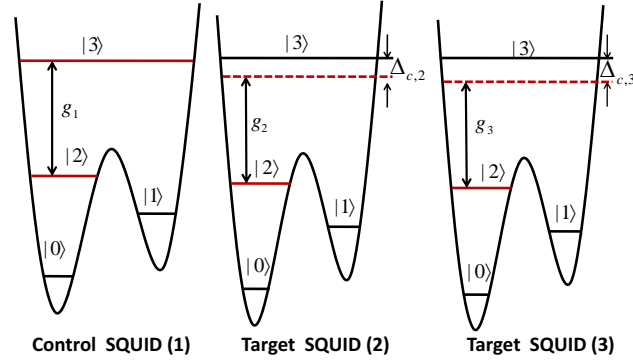


FIG. 2: Level diagram of control SQUID and target SQUIDs with four levels $|0\rangle$, $|1\rangle$, $|2\rangle$, and $|3\rangle$. The levels $|2\rangle$, and $|3\rangle$ of control SQUID interact resonantly to resonator while levels $|2\rangle$ and $|3\rangle$ of each target SQUID interact off-resonantly to the resonator. The difference between level spacing of each SQUID can be achieved by choosing different device parameters for SQUIDs.

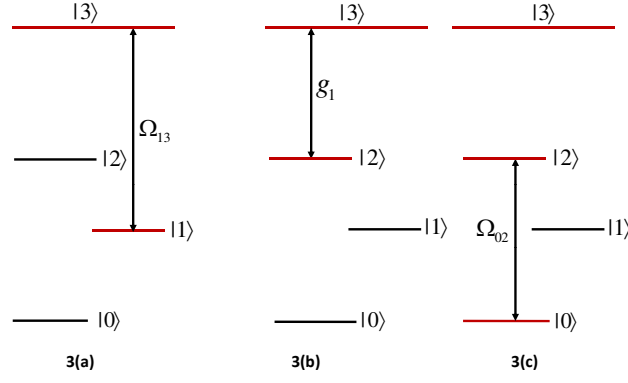


FIG. 3: Illustration of control SQUID(1) interacting with the resonator mode and/or the microwave pulses during the gate operation.

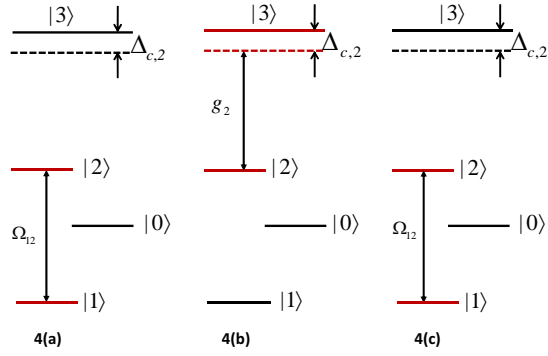


FIG. 4: Illustration of target SQUID(2) interacting with the resonator mode and/or the microwave pulses during the gate operation.

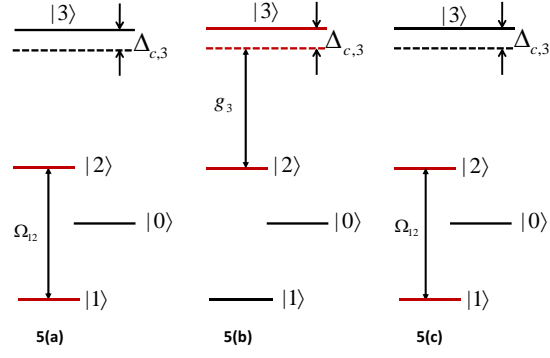


FIG. 5: Illustration of target SQUID(3) interacting with the resonator mode and/or the microwave pulses during the gate operation.

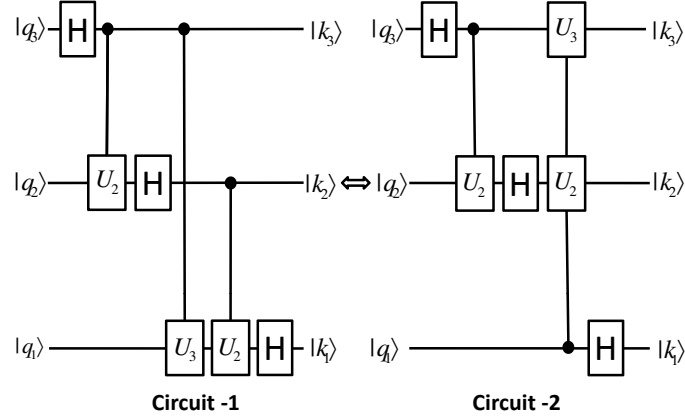


FIG. 6: Circuit-1 is a schematic network for three qubit QFT. The states $|q_n\rangle$ and $|k_n\rangle$ ($n = 1, 2, 3$) represent inputs and outputs, respectively. Here H represents Hadamard transformation and U_n two-qubit conditional phase transformation. The filled circles represent the control qubits. Using the equivalent circuit shown in Fig. 1., circuit-1 reduces to circuit-2.

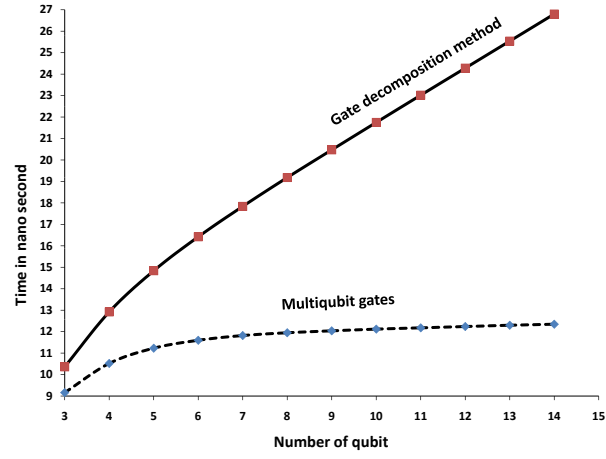


FIG. 7: Plot of the gate implementation time against the number of qubits.